Available online at www.sciencedirect.com
SCIENCE DIRECT
Geomorphology 76 (2006) 430–440
GEOMORPHOLOGY
www.elsevier.com/locate/geomorph

Quantifying sediment transport across an undisturbed prairie landscape using cesium-137 and high resolution topography

James M. Kaste [a,*], Arjun M. Heimsath [a], Matthew Hohmann [b]

[a] *Department of Earth Sciences, 6105 Fairchild Hall, Dartmouth College, Hanover, NH 03755, USA*
[b] *U.S. Army Engineer Research and Development Center, Construction Engineering Research Laboratory, PO Box 9005, Champaign, IL 61826-9005, USA*

Received 20 June 2005; received in revised form 7 December 2005; accepted 9 December 2005
Available online 17 February 2006

Abstract

Soil erosion is a global environmental problem, and anthropogenic fallout radionuclides offer a promising tool for describing and quantifying soil redistribution on decadal time scales. To date, applications of radioactive fallout to trace upland sediment transport have been developed primarily on lands disturbed by agriculture, grazing, and logging. Here we use ^{137}Cs to characterize and quantify soil erosion at the Konza Prairie Long-Term Ecological Research (LTER) site, an undisturbed grassland in northeastern Kansas. We report on the small scale (<10 m) and landscape scale (10 to 1000 m) distribution of fallout ^{137}Cs, and show significant variability in the concentrations and amounts of ^{137}Cs in soils at our site. ^{137}Cs soil concentrations and amounts typically vary by 10% to 30% on small scales, which most likely represents the spatial heterogeneity of the depositional processes. Landscape scale variability of soil ^{137}Cs was significantly higher than small scale variability. Most notably, soils collected on convex (divergent) landforms had ^{137}Cs inventories of 2500 to 3000 Bq m^{-2}, which is consistent with the expected atmospheric inputs to the study area during the 1950s and 1960s. Concave landforms, however, had statistically lower inventories of 1800 to 2300 Bq m^{-2}. The distribution of ^{137}Cs on this undisturbed landscape contrasts significantly with distributions observed across disturbed sites, which generally have accumulations of radioactive fallout in valley bottoms. Because the upslope contributing area at each sampling point had a significant negative correlation with the soil inventory of ^{137}Cs, we suggest that overland flow in convergent areas dominates soil erosion at Konza on time scales of decades. Very few points on our landscape had ^{137}Cs inventories significantly above that which would be predicted from direct deposition of ^{137}Cs on the soil surface; we conclude therefore that there is little net sediment storage on this undisturbed landscape.

Keywords: Erosion; Overland flow; Konza Prairie; Grassland; Geomorphology

1. Introduction

Each year the world loses billions of tons of soil from erosion, a flux that is likely to exceed natural soil production rates (Pimentel et al., 1995). Soil erosion has been accelerated in recent years from cultivation, logging, and other effects of anthropogenic manipulation of the landscape (Hooke, 2000; Hewawasam et al., 2003). As soil is transported off of the land surface, it can damage aquatic ecosystems (Osmundson et al., 2002) and it can reduce this global resource for food, fiber, and timber production. A detailed understanding of soil erosion across different types of landscapes is critical, therefore, for developing sustainable land management practices.

* Corresponding author.
E-mail address: James.Kaste@Dartmouth.edu (J.M. Kaste).

0169-555X/$ - see front matter © 2005 Elsevier B.V. All rights reserved.
doi:10.1016/j.geomorph.2005.12.007

Quantifying soil production and transport rates and processes is, however, difficult and resource intensive. Long-standing efforts to determine average erosion rates across agricultural landscapes involve the construction of small-scale runoff plots (Roels, 1985), monitoring of suspended sediment concentrations in streams draining the landscapes (Steegen et al., 2001), and, with recent analytical breakthroughs, through the use of sediment tracers (Matisoff et al., 2001) or short-lived isotopes (Matisoff et al., 2002a,b). Collection and analyses of soil from runoff plots or suspended sediment analyses remains problematic primarily because of the difficulties with ensuring a closed system, while injection of tracers onto agricultural lands immediately imparts a short-term measurement bias. Soil production rates have been determined for diverse upland landscapes using in situ produced cosmogenic nuclides (Heimsath et al., 1997), but the methodology depends on local steady state soil thickness and is therefore not appropriate for agricultural land or where soil depths are greater than about a meter. Attempts to quantify sediment transport processes include segmented rod studies (Young, 1960), tephra deposit mapping (Roering et al., 2002), detailed measurement of bioturbation (Black and Montgomery, 1991; Gabet, 2000), optically stimulated luminescence dating of individual quartz grains (Heimsath et al., 2002), and short-lived isotope measurements (Wallbrink and Murray, 1996; Walling and He, 1999a,b). Despite the extensive effort across disciplines, quantifying sediment transport processes and rates remains elusive (Dietrich et al., 2003).

During the middle of the twentieth century, the detonation of nuclear weapons in the atmosphere injected a host of artificial radionuclides into the environment with half-lives ranging from days to decades. While atmospheric weapons were tested in various countries from the 1940s until the late 1970s, the vast majority of fallout in the central United States was deposited between 1955 and 1967 (Cambray et al., 1989; Simon et al., 2004). These fallout radionuclides offer a unique tool for determining time-integrated erosion rates on a landscape with only one or a few visits to the site (Brown et al., 1981b; Zhang et al., 1994; Quine et al., 1997; Walling et al., 1999, 2002; He and Walling, 2003; Porto et al., 2003; Fornes et al., 2005). ^{137}Cs has a relatively long half-life (30 yr), it binds strongly to illite-like clay minerals (Lomenick and Tamura, 1965), and is relatively simple to measure via its strong gamma emission at 662 keV. This makes it ideal for studying soil redistribution at certain sites. The technique relies on the assumption that the isotope is fixed to particles upon deposition, and any redistribution of ^{137}Cs represents erosion and deposition on the landscape. Areas on the landscape with relatively high amounts of ^{137}Cs are assumed to be areas of aggradation, and areas with relatively low amounts of ^{137}Cs are assumed to result from topsoil erosion. Elaborate models have been developed for relating the vertical distribution of radioactive fallout in soil profiles and aerial amounts of radiocesium at different points on the landscape to erosion rates (Walling and He, 1999a).

The techniques of relating ^{137}Cs profiles and inventories to absolute and relative erosion rates commonly relies on finding a "non-eroding" reference location to compare to eroding or aggrading sites (Lowrance et al., 1988). Nearly all erosion studies of this type compare soils sampled at cultivated sites with those sampled from an undisturbed field or forest. A considerable problem in relating the inventories of radioactive fallout to an actual erosion rate is the spatial heterogeneity of the fallout deposition. Only a few works have intensively studied the variability of ^{137}Cs at undisturbed landscapes that are often taken as reference locations (Lance et al., 1986; Sutherland, 1994,1996; Owens and Walling, 1996; VandenBygaart et al., 1999).

Here we examine the distribution of ^{137}Cs on a prairie landscape that has remained relatively free from anthropogenic disturbance. Our goals are to quantify the small-scale variability (<10 m) of ^{137}Cs in soils and to ascertain if basin-scale (10 to 1000 m) variability exceeds small-scale variability. In addition, we test whether topographical attributes such as slope, curvature, and upslope contributing area are related to ^{137}Cs inventories, and use these relationships to gain insight into the erosion processes occurring on this landscape over the past four decades.

2. Study area

Our study site is a 455, 400-m^2 rectangular plot of the Konza Prairie in Geary County, part of the Flint Hills region of northeastern Kansas (Fig. 1). The site is part of a region encompassing 50,000 km^2 of eastern Kansas and northeastern Oklahoma, and constitutes a part of the largest remaining area of unplowed tallgrass prairie in North America. Konza land was used for cattle grazing (horses, hogs, mules, cattle) in the early 1900s, but has been managed as a Long-Term Ecological Research (LTER) site since the 1970s. Its current management includes periodic burns and the reintroduction of native grazers (bison).

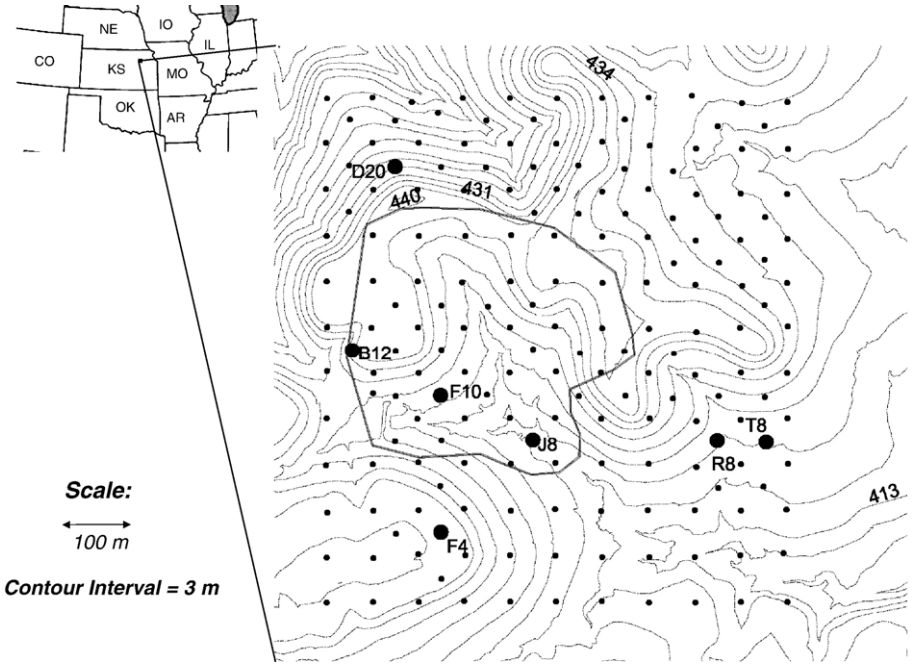

Fig. 1. Konza Prairie field site. Small points mark single core locations; large points mark subsampling plots where four additional cores were taken every 1, 5, and 10 m surrounding the grid point (see Fig. 2).

The vegetation of the study site is mostly native tallgrass prairie, dominated by the perennial warm-season grasses, including big bluestem (*Andropogon gerardii* Vitman), Indiana grass (*Sorghastrum nutans* (L.) Nash), little bluestem (*Schizachyrium scoparium* Michx.) and switch grass (*Panicum virgatum* L.). Trees and shrubs can be found on slopes that do not regularly burn (Briggs et al., 2002). The most common tree and shrub species found on slopes include American elm (*Ulmus Americana* L.), honeylocust (*Gleditsia triacanthos* L.), hackberry (*Celtis occidentalis* L.), redcedar (*Juniperus virginiana* L.), and dogwood (*Cornus drummondii* L.).

Most of the study site lies in an area having soils classified as Benfield–Florence complex, which consists of Benfield silty clay and Florence cherty silt loam complex. Soils are developed on flat-lying Permian carbonates and shales, and soil texture has been measured as ~50% silt, 30% clay, and 20% sand (Macpherson and Sophocleous, 2004). Small portions near the NW and NE boundaries of the study site have soils classified as Crete silty loam and Tully silty clay loam, respectively.

The study site spans three watersheds, with each having different grazing and burn regimes. The northwestern corner of the study site lies within watershed SB, which is ungrazed and not subject to prescribed burns. The majority of the site lies within watershed C4A, which is grazed by cattle and has a 4-yr fire return interval. The southernmost portion of the study site lies within watershed C1B, which is burned every year and is also subject to cattle grazing. Most prescribed burns within the study site occur during the end of the dormant period in April. The climate for the area is temperate

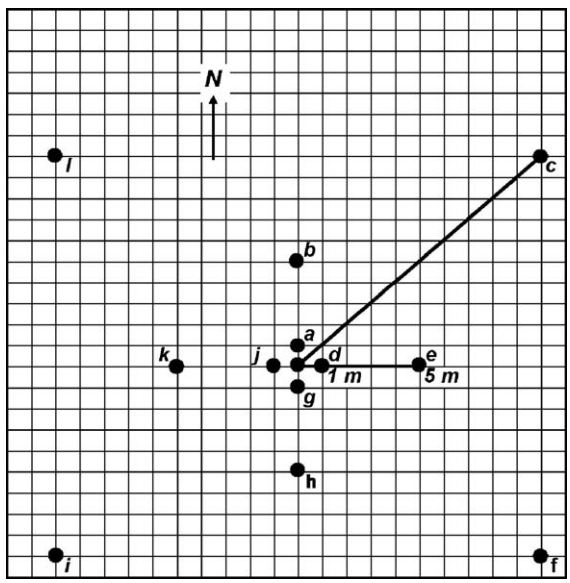

Fig. 2. Subsampling design for plots identified in Fig. 1. Each grid cell represents 1 m^2.

midcontinental: rainfall averages 83.5 cm/year, of which approximately 75% occurs in the growing season from April through September. Mean January temperature is −2.7 °C and mean July temperature is 26.6 °C.

3. Methodology

3.1. Soil sampling

A 660-m × 690-m sampling grid was used to define our study site and identify sampling points (Fig. 1). Soils were sampled in the Spring of 2003 at 60-m spacing. We used a coring device that retrieved soil in a 43-mm-ID × 303-mm-long plastic tube. To ascertain the small-scale variability of ^{137}Cs, selected locations that represent different landscape positions (hilltops, slopes, valleys) were subsampled at higher resolution (Figs. 1 and 2), with four additional cores taken at 1, 5, and 10-m intervals around the original sampling point. Because others have described the vertical distribution of ^{137}Cs in soil cores from the Konza Prairie (Reguigui and Landsberger, 2005), we focused our resources on quantifying the spatial distribution of ^{137}Cs on the landscape. Reguigui and Landsberger (2005) demonstrated that >90% of the ^{137}Cs resides in the upper 20 cm of soil at the Konza Prairie. All extracted soil from the core tubes was bulked for each sampling point. We also sampled grass at the site to determine the relative significance of ^{137}Cs cycling by the native vegetation. Grasses were clipped above ground and stored in plastic bags for radionuclide analysis.

3.2. Radionuclide analysis

Sieved (<2 mm) soil samples and ground grass samples were oven-dried at 105 °C and packed into plastic containers for ^{137}Cs analysis via its 662 keV gamma emission. Depending on the mass of sample retrieved, soils were packed either in a 60 or 125 ml geometry that was calibrated with standard ^{137}Cs solutions (Isotope Products). We used two Canberra Broad Energy Intrinsic Ge Detectors for gamma analysis, each equipped with a low-background lead shield. Efficiency of the detectors for the ^{137}Cs gamma ranged from 2% to 4%, depending on the precise geometry and the specific detector. We typically counted samples for 80 ks, accumulating ~1000 counts in order to keep the random error associated with gamma and X-ray spectrometry below 3%. ^{137}Cs concentrations in soil (Bq kg^{-1}) were calculated by correcting for the detector efficiency and the efficiency of the ^{137}Cs 662 keV gamma emission (85% yield). ^{137}Cs inventories (Bq m^{-2}) were estimated by multiplying the concentration of ^{137}Cs in the soil by the total mass of soil retrieved by the coring device. Repeat analysis of samples and quality control checks indicated that the error associated with our gamma analysis (1 standard error) was on the order of 6%.

3.3. Topographical analysis

We developed a high resolution digital elevation model (DEM) for the study site using a photogrammetric approach that would ensure a vertical accuracy associated with 0.6-m contour interval as stated in the National Map Accuracy Standards (NMAS). Prior to aerial photography, six semi-permanent targets were placed in the study area to be used as subsequent ground control points for orienting the photogrammetric models. On 01 October 2003, black and white aerial photography was flown over the study area at an altitude of 1066 m (above mean terrain). A Zeiss RMK 23/15 precision aerial camera with forward motion compensation and airborne global positioning system (GPS) was used to acquire the photos. The resolution of the camera lens had an area weighted average resolution (AWAR) of 90 line pairs per millimeter as determined by a USGS calibration report from June 2003. Negatives were scanned into a digital format using a 20-μ scan resolution on a Vexcel 5000 photogrammetric scanner.

Data on the location and elevation of the targets and additional photo-identifiable ground control points were collected with Trimble® GPS receivers and post-processed with GPsurvey® and GEOlab® software. Survey points were tied to the "KAW" and "N 370" stations of the National Geological Survey (NGS) control monumentation. Aerial triangulation was performed with Z/I Imaging ISAT software to verify the ground control points and supplement the photogrammetric model setups. Map compilation of the high resolution DEM was collected on Z/I Imaging SSK photogrammetric workstations. In order to verify the accuracy of the DEM, additional field check points were surveyed at 47 random locations throughout the study area and compared with photogrammetric estimates. The mean square error resulting from the elevation differences was 5.2 cm, which is well within the 95% confidence range for a 0.6-m elevation accuracy. SHALSTAB (Dietrich et al., 1995; Montgomery and Dietrich, 1994) was used to calculate slope, curvature, and upslope contributing area across our grid. We used a 7-m grid scale for the topographical analyses, which appeared to be the lowest resolution free of artifacts in the curvature displays.

Table 1
^{137}Cs concentrations (Bq kg^{-1}) and inventories (Bq m^{-2}) determined on subsampled plots

1 m	^{137}Cs Bq kg^{-1} (Bq m^{-2})	5 m	^{137}Cs Bq kg^{-1} (Bq m^{-2})	10 m	^{137}Cs Bq kg^{-1} (Bq m^{-2})
B12	15.8 (3730)				
B12a	20.0 (4010)	B12b	8.53 (2050)	B12c	12.4 (3240)
B12d	11.1 (3010)	B12e	13.8 (3450)	B12f	NA (NA)
B12g	14.1 (2540)	B12h	17.7 (3670)	B12i	7.49 (2780)
B12j	10.7 (2690)	B12k	14.2 (1640)	B12l	5.68 (2150)
1 m: 3200±20%		1+5 m: 2980±27%		1+5+10 m: 2910 ±25%	
D20	10.8 (2550)				
D20a	8.86 (3040)	D20b	5.31 (1930)	D20c	10.6 (3710)
D20d	14.5 (4220)	D20e	12.1 (4060)	D20f	6.85 (2310)
D20g	8.32 (2800)	D20h	5.38 (1870)	D20i	5.37 (1770)
D20j	8.67 (2300)	D20k	6.74 (2380)	D20l	6.66 (2080)
1 m: 2980±25%		1+5 m: 2790±30%		1+5+10 m: 2690 ±31%	
F4	9.75 (3120)				
F4a	11.1 (3780)	F4b	11.3 (3730)	F4c	13.9 (3670)
F4d	5.91 (1790)	F4e	10.8 (3580)	F4f	9.12 (2820)
F4g	11.1 (3600)	F4h	12.2 (4200)	F4i	11.0 (3200)
F4j	10.3 (3100)	F4k	11.2 (3970)	F4l	5.67 (1790)
1 m: 3080±25%		1+5 m: 3430±21%		1+5+10 m: 3260 ±23%	
F10	4.76 (1630)				
F10a	6.42 (2360)	F10b	12.6 (4750)	F10c	6.62 (2700)
F10d	6.35 (1920)	F10e	7.69 (2550)	F10f	5.43 (1730)
F10g	5.18 (1880)	F10k	5.02 (1840)	F10i	7.87 (2910)
F10j	6.06 (2260)	F10h	4.07 (1620)	F10l	7.52 (2710)
1 m: 2010±17%		1+5 m: 2310±42%		1+5+10 m: 2370 ±39%	
J8	6.25 (1780)				
J8a	6.10 (1640)	J8b	3.10 (870)	J8c	4.32 (1190)
J8d	5.48 (1750)	J8e	4.76 (1780)	J8f	5.46 (1830)
J8g	6.00 (2220)	J8h	6.62 (2030)	J8i	5.41 (1740)
J8j	6.43 (1810)	J8k	5.38 (1870)	J8l	3.90 (1360)
1 m: 1840±14%		1+5 m: 1750±24%		1+5+10 m: 1680 ±23%	
R8	6.92 (2300)				
R8a	10.3 (1960)	R8b	6.23 (2030)	R8c	5.34 (2050)
R8d	5.66 (2110)	R8e	4.33 (1480)	R8f	6.90 (2580)
R8g	6.35 (2260)	R8h	4.36 (1650)	R8i	5.70 (2080)
R8j	6.19 (1650)	R8k	5.33 (1790)	R8l	3.98 (1600)
1 m: 2060±8%		1+5 m: 1910±16%		1+5+10 m: 1960 ±16%	
T8	7.32 (2280)				
T8a	5.36 (1700)	T8b	5.40 (1910)	T8c	7.46 (2490)
T8d	5.74 (1950)	T8e	5.99 (2200)	T8f	4.82 (1830)
T8g	6.90 (2200)	T8h	6.47 (2040)	T8i	4.58 (1610)
T8j	5.99 (1910)	T8k	3.66 (1380)	T8l	5.08 (1780)
1 m: 2010±13%; ;		1+5 m: 1950±10%		1+5+10 m: 1940 ±14%	

Averages and standard errors are given for inventory values.

4. Results and discussion

4.1. Subsampling

Table 1 gives soil ^{137}Cs concentrations (Bq kg^{-1}) and amounts (Bq m^{-2}) from our small scale subsampling plots (Fig. 2). Soil concentrations typically show a wider range of variability than surface inventories because concentrations are effected by the depth and amount of soil collected by the coring device. Since radioactive fallout is concentrated in the upper soil horizons, the retrieval of a thicker soil column will result in dilution of the isotope. Surface inventories (Bq m^{-2}) are thus more useful for geomorphic and sediment transport studies. Within all of the subsample plots, analysis of variance (ANOVA) tests using Tukey Kramers HSD could not distinguish between 1-, 5-, and 10-m data ($\alpha = 0.05$). The variability about the mean of each sampling point increases significantly if 5-m data is included with the 1-m data; variability increases even more if the 10-m data is included with the 1- and 5-m data. However, when all of the subsamples are used for comparison between the subsampling plots, ANOVA indicated that J8, R8, and T8 are significantly lower in ^{137}Cs (Bq m^{-2}) than B12, D20, F4, and F10 at $\alpha = 0.05$. Subsamples J8, R8, and T8 were all located in convergent regions of landscape and have positive curvature, while subsamples B12, D20, F4, and F10 were on sites with negative curvature (convex regions).

4.2. Landscape distribution of ^{137}Cs

^{137}Cs inventories measured in our grid at Konza (not including subsamples) ranged from 800 to 3900 Bq m^{-2} ($\pm 2\sigma, n = 189$). Fig. 3 gives ^{137}Cs amounts (Bq m^{-2}) versus slope, and no significant correlation exists between these two parameters. Significant correlations with topographic curvature (linear; $p < 0.001$) and upslope contributing area (logarithmic; $p < 0.001$) are

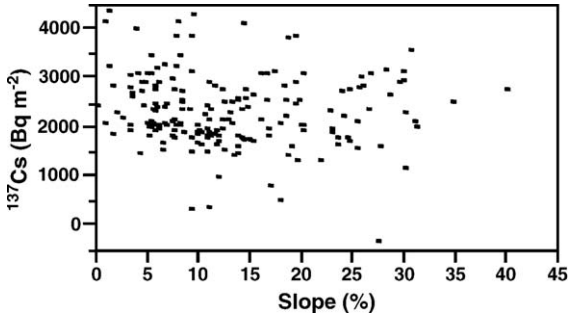

Fig. 3. ^{137}Cs inventory vs. slope calculated at the 7-m grid scale for the entire sampling grid. No significant correlation exists.

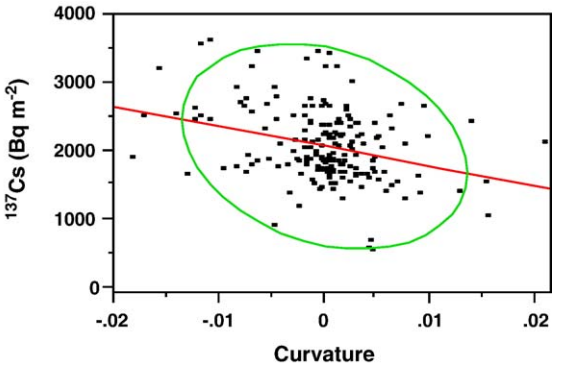

Fig. 4. ^{137}Cs inventory vs. curvature calculated at the 7-m grid scale for the entire sampling area. Confidence interval density ellipse is given as 95%. A significant correlation exists here ($p<0.001$); r^2 on the linear fit (given) is 0.07.

shown in Figs. 4 and 5, respectively. If samples are grouped according to curvature, sites with negative curvature (−0.03 to −0.005) have statistically higher ^{137}Cs soil concentrations and amounts than sites that are flat or positive in curvature (concave) (Fig. 6).

4.3. Comparison with other studies

The distribution of ^{137}Cs on this landscape is very different than the ^{137}Cs distributions commonly described on cultivated landscapes. While we show ^{137}Cs depletion in concave areas, most disturbed sites have significant ^{137}Cs enrichments downslope. Brown et al. (1981a) reported on the distribution of ^{137}Cs in agricultural watersheds in Oregon. They reported that

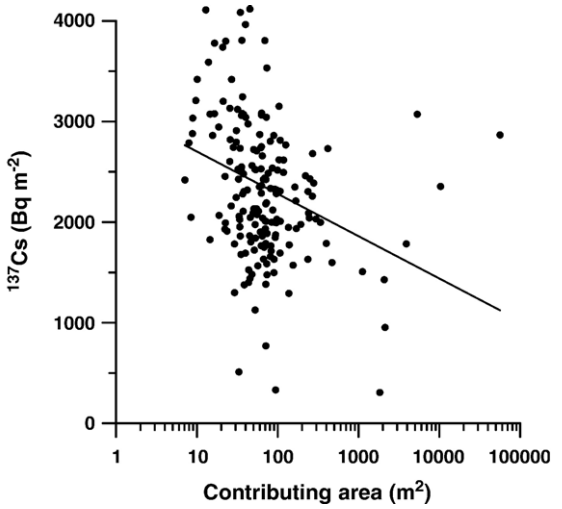

Fig. 5. ^{137}Cs inventory vs. upslope contributing area (m^2) calculated at the 7-m grid scale for the entire sampling grid. A significant correlation exists here ($p<0.001$); r^2 on the logarithmic fit (given) is 0.07.

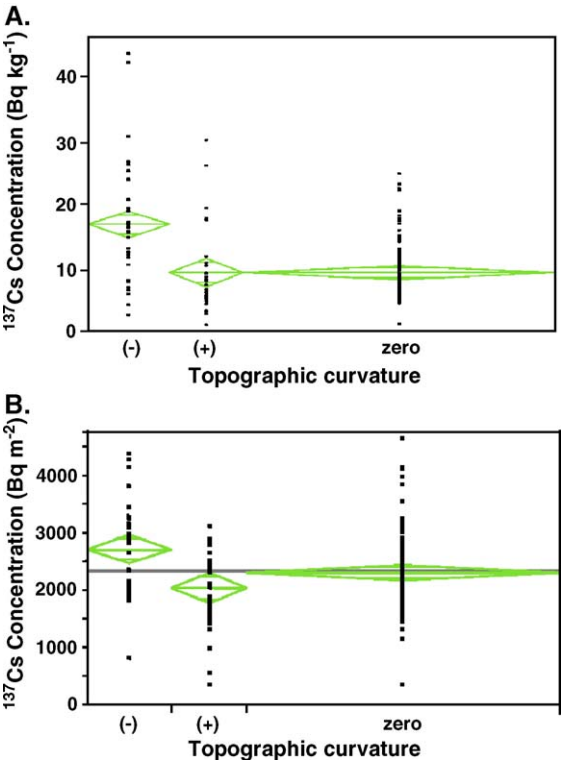

Fig. 6. ^{137}Cs concentrations (A) and surface inventories (B) grouped by topographic curvature. Negative curvature ranges from −0.03 to −0.005. Zero curvature ranges from −0.005 to +0.005. Positive curvature ranges from +0.005 to +0.03. An ANOVA shows that sampling locations with negative curvature are statistically different ($\alpha=0.05$) from zero and positive curvature.

sideslopes and ridgetops had ^{137}Cs inventories ranging from 1500 to 2500 Bq m^{-2}. Concave footslope positions had significantly higher ^{137}Cs inventories, ranging from 2500 to 3800 Bq m^{-2}. At a tilled watershed in Oklahoma, Lance et al. (1986) also showed significant downslope enrichments of ^{137}Cs relative to midslope or ridge crest positions. Martz and De Jong (1987) used ^{137}Cs to describe the relationship of soil erosion in a cultivated prairie basin in central Saskatchewan. They also concluded that soil loss was most severe on slope crests, and soil accumulation was reported in upland depressions and along the main valley channel. Lowrance et al. (1988) analyzed the distribution of ^{137}Cs in a cultivated field in Georgia. They determined that hillslopes were eroding at rates of ~60 Mg ha^{-1} y^{-1}, and this sediment was being deposited and temporarily stored in downslope areas of the field and in a riparian forest ecosystem. Hillsopes had ^{137}Cs inventories of ~1600 Bq m^{-2}, whereas soils and sediments in the riparian forest and toeslopes had higher inventories by about sixfold. Walling et al.

(1999) examined the spatial distribution of radiocesium on a cultivated field in England. They showed that hilltops and hillslopes had ^{137}Cs inventories ranging from 1800 to 2300 Bq m^{-2}. Valley bottoms, however, had significantly higher amounts of ^{137}Cs by a few hundred becquerels per square meter. Riparian areas also appeared to trap and accumulate ^{137}Cs (and presumably sediment) eroded from cultivated hillslopes in western Slovakia (Van der Perk et al., 2002).

The spatial variability of ^{137}Cs in undisturbed areas has not been documented as rigorously, although it appears to be significantly lower than the variability at disturbed locations. At an undisturbed watershed in Oklahoma, Lance et al. (1986) found that the coefficient of variation (CV) was 19%, lower than in the nearby cultivated basin that had a ^{137}Cs CV of 33%. Sutherland (1994) reported a CV of 28% for a cultivated field in Saskatchewan, compared to a 15% CV in a nearby native field. Interestingly, for the native field control site he concluded that all ^{137}Cs inventories in downslope transects had a random distribution, although a ^{137}Cs depleted area was noted in a topographical hollow.

In a subsequent literature review of the use of ^{137}Cs reference locations, Sutherland (1996) reported that the CV of ^{137}Cs inventories in undisturbed and presumably noneroding and nonaggrading soil ranged from 13% to 23% (95% confidence interval). Navis and Walling (1992) demonstrated that land use was a much more significant factor in determining ^{137}Cs inventories than topography. Areas with natural vegetation and relatively steep slope (15°) had higher amounts of ^{137}Cs than more gentle slopes (5°) that were cultivated. Owens and Walling (1996) calculated a CV of 18% and 67% for ^{137}Cs inventories at an undisturbed orchard in the U.K. and a grassland in Zimbabwe, respectively. They concluded that most of the variability at these low-gradient sites was random. While the overall CV at Konza was relatively high (33%), the CV within a very small scale (all samples <1 m) ranged from 8% to 25%. If samples were grouped around a diameter of 20 m the CV was as high as 39% (Table 1). ^{137}Cs inventories within the Konza sampling grid are significantly correlated with landscape curvature and upslope contributing area (Figs. 4–6).

5. Tracing soil redistribution and quantifying erosion across a natural prairie

Although ^{137}Cs can move in soils in both particulate and dissolved form (Tyler and Heal, 2000), soils and sediments with low organic matter and significant clay content generally have low dissolved ^{137}Cs losses (Lomenick and Tamura, 1965; Seaman et al., 2001; Smith et al., 2004). Konza soils have clay contents on the order of 20% to 30%, and organic matter concentrations of <10% (Dell et al., 2005; Dodds et al., 1996; Macpherson and Sophocleous, 2004), thus ^{137}Cs should be relatively immobile at this site. Over 90% of the ^{137}Cs at Konza resides in the upper 15 cm of soil (Reguigui and Landsberger, 2005). The vertical distribution of ^{137}Cs is in broad agreement with the distribution of fallout Plutonium (Pu) at Konza (Fig. 7), which has also been documented to be strongly partitioned to the solid phase (Santschi et al., 1980). While preferential leaching of ^{137}Cs relative to other fallout isotopes is observed in organic-rich soils (Dorr and Munnich, 1991), we did not observe this at Konza (Fig. 7). In addition, in our analyses of vegetation, ^{137}Cs uptake was very low; ^{137}Cs inventories in the grasses ranged from 10 to 50 Bq m^{-2}, which is relatively insignificant compared to soil inventories that range from 1800 to 3500 Bq m^{-2}. Because of our soil texture, the depth-distribution of ^{137}Cs, and the low ^{137}Cs uptake by vegetation, we feel that it is justified to assume that ^{137}Cs movement at Konza is dominated by particulate transport.

Using the spatial distribution of fallout ^{137}Cs at Konza, we can describe the soil redistribution and erosion that has taken place over the last few decades.

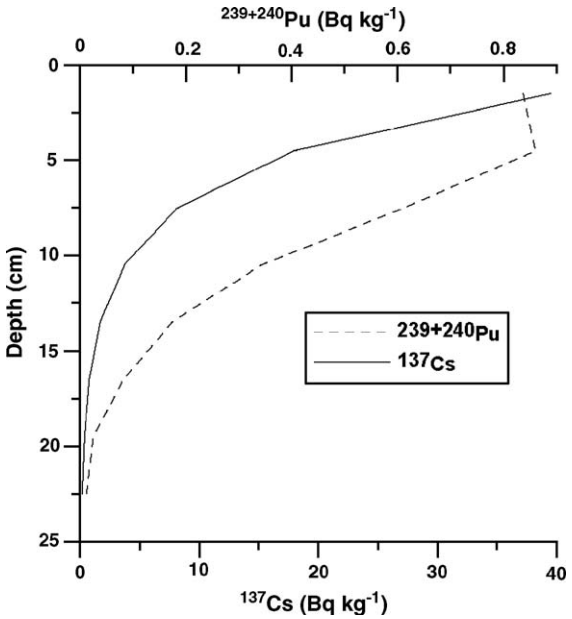

Fig. 7. Vertical distribution of ^{137}Cs and Pu fallout at Konza. ^{137}Cs data generalized from Reguigui and Landsberger (2005); Pu determinations were by M.E. Ketterer at Northern Arizona University.

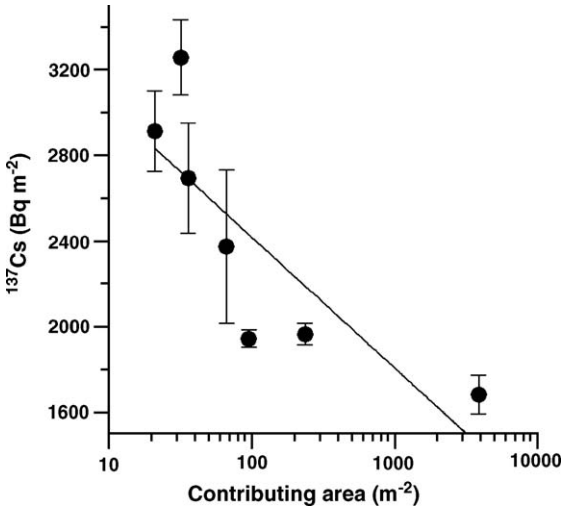

Fig. 8. ^{137}Cs inventories vs. upslope contributing area for the subsamples given in Table 1. Averages of the 1- and 5-m samples plotted +/−1 standard error of the mean. The r^2 on the log fit (plotted) is 0.7.

^{137}Cs inventories at our site ranged ($\pm 2\sigma, n=189$) from 800 to 3900 Bq m^{-2}. Sampling points on convex landforms had ^{137}Cs values of 2450 to 3020 (95% CI) and soil sampled from flat areas (i.e., no curvature) had ^{137}Cs values of 2190 to 2440 (95% CI). These values are relatively consistent with depositional models of ^{137}Cs fallout to northeastern Kansas during the 1950s and 1960s (Simon et al., 2004). However, soil sampled from concave landforms had 1720 to 2370 Bq ^{137}Cs m^{-2} (95% CI), and these locations were significantly lower than convex areas.

Because convex landforms have ^{137}Cs inventories consistent with inventories predicted by local and global fallout, erosional processes must operate on a time scales >40 yr here. However, from subsampling locations ($n=13$ in areas <20 m) and from the larger grid survey (Fig. 1), concave topography had soil ^{137}Cs inventories below that of convex topography. Furthermore, while ^{137}Cs inventories show no relationship with slope (Fig. 3), a negative logarithmic relationship exists with contributing area (Fig. 5). When all samples are considered (Fig. 5), the relationship between ^{137}Cs inventories and contributing areas is weak, probably because most of the sampling points are clustered between 10 and 100 m^2 and because of the 10% to 25% error associated with each sampling point (Table 1). A much tighter correlation can be found among the subsampling averages and upslope contributing area (Fig. 8). In addition, when individual watersheds are isolated, a tighter correlation between ^{137}Cs inventories and upslope contributing area is found (Fig. 9). From the ^{137}Cs concentration and inventory data, soil erosion at Konza appears to be occurring in areas that focus surface water flow.

In addition to using ^{137}Cs to identify areas of soil loss, soil loss can be quantitatively assessed for concave portions of the landscape if we assume that: i) the convex sampling locations have not been eroding and can serve as our reference inventory, and ii) the vertical distribution of fallout ^{137}Cs at Konza is of the exponential form shown by Reguigui and Landsberger (2005). We use a model based on Walling and He (1999a) that relates the percentage of ^{137}Cs loss

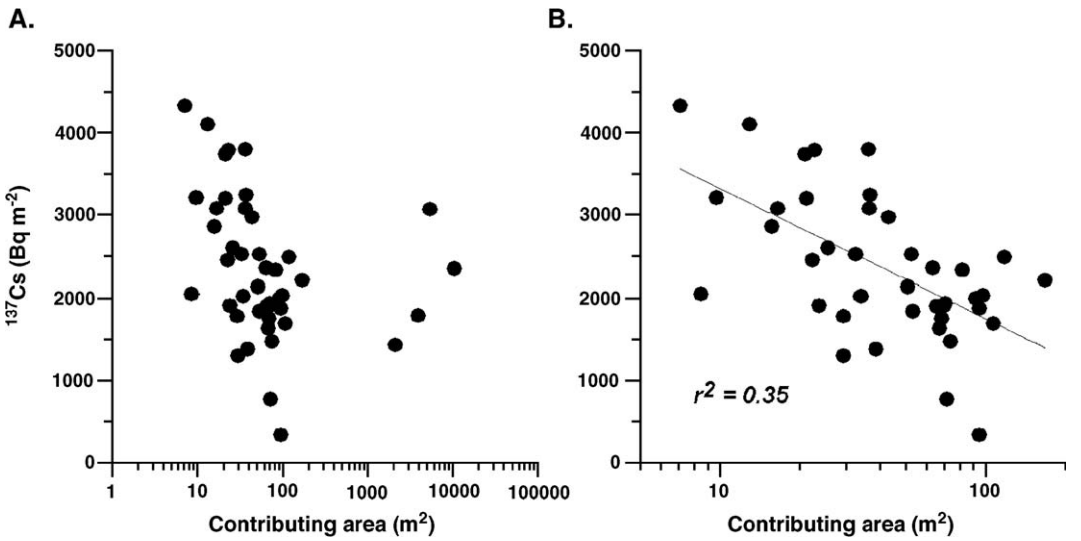

Fig. 9. ^{137}Cs inventories vs. contributing area for the watersheds circled in Fig. 1. Plot B omits all data points (4) with >150 m^2 contributing area. r^2 on the logarithmic fit (given) is 0.35.

(relative to reference inventory) to soil erosion rates using parameters that govern the vertical distribution of ^{137}Cs in the soil. The model takes into account the advection (i.e., leaching) and dispersion (e.g., mixing) of ^{137}Cs in the soil profile and the time-dependent ^{137}Cs fallout input function. In the model, we also assume that mobilized sediment is enriched by a factor of 1.2 in ^{137}Cs relative to topsoil because of preferential removal of fines that have a larger reactive surface area for ^{137}Cs adsorption (He and Walling, 1996). Concave landforms have ^{137}Cs depletions ranging from 13% to 37%, which translates to erosion rate estimates of 1 to 2.5 Mg ha^{-1} y^{-1}.

Recent soil erosion at the Konza Prairie is focused in convergent areas, while convex landforms have remained stable. Because upslope contributing area has the most significant correlation with ^{137}Cs inventories, we conclude that overland flow has been the dominant erosion process on the landscape over the last 40 yr. Discharge is a function of upslope contributing area, thus net sediment transport is localized to portions of the surface that are subjected to shear stress sufficient for particle entrainment. Others have documented overland flow on low gradient grassland slopes. For example, Montgomery and Dietrich (1989, 1994) observed overland flow in convergent areas on grasslands in Marin County, California, and connected the increased transport capacity with channel initiation. Their work led to field experiments testing the role of vegetative strength with channel formation and found surprising resilience of grassland landscapes to overland flow erosion (Prosser and Dietrich, 1995). A significant conclusion from such studies is that land management, specifically determining the species of grazing animals and nature of tillage agriculture, can alter the rates and processes of erosion tremendously. Although a comprehensive comparison of management strategies is beyond the scope of this paper, the erosion rates that we calculated for concave landforms are significantly lower than hillslope erosion rates calculated at topographically similar cultivated sites using fallout isotopes, which generally range from 2 to >100 Mg ha^{-1} y^{-1} (Brown et al., 1981b; Fornes et al., 2005; Lance et al., 1986; Lowrance et al., 1988; Martz and De Jong, 1987; Wilson et al., 2003).

While we report net erosion at Konza, resulting primarily from overland flow removal of sediment from the unchannelled swales, little evidence was found of net deposition or sediment storage on this landscape. Out of the 30 sampling points in concave areas, which generally lie in valley bottoms, only one point had ^{137}Cs>3500 Bq m^{-2}. Sites with little to no curvature (n=125) had ^{137}Cs inventories generally consistent with expected ^{137}Cs deposition. This sharply contrasts with cultivated sites, which almost always have significant accumulations of ^{137}Cs, often several times the reference inventory at the base of slopes as discussed above. This study thus sheds light on the sediment transport in a basin in its "natural condition" and one that is often presumed to be at steady state. Any sediment produced appears to be exported from the system, possibly stored down gradient outside of our study area. We demonstrated here that low-order watersheds on undisturbed grasslands have a sediment delivery ratio (e.g., transmission ratio) near 100%.

6. Conclusions

While it is often assumed that ^{137}Cs amounts would not vary significantly across an undisturbed landscape, we demonstrated that ^{137}Cs concentrations and surface inventories span a significant range even on a scale of a few meters at natural grassland in Konza. Using ^{137}Cs inventories, we documented erosion on this landscape and showed that the erosion is confined to convergent regions. Because the topographical attribute that has the most significant relationship with ^{137}Cs inventories is the upslope contributing area, we suggest that overland flow is the dominant erosive process operating here on time scales of decades. ^{137}Cs inventories in our sampling grid are generally consistent with or below inventories expected from atmospheric inputs during the middle-to-late 20th century. We conclude that there is little net sediment storage at this undisturbed prairie, which contrasts sharply from disturbed landscapes.

Acknowledgements

We thank Tyra Olstad, who assisted with the gamma-ray spectrometry, and Larry Gatto for coordinating this project and helping to collect the samples. Western Air Maps shot the aerial photography and generated the high resolution DEM. We also thank Michael E. Ketterer for providing us with plutonium measurements. William Johnson and Gwen Macpherson helped with sampling, project design, and sample processing. Andrew Elmore and Heather Carlos helped with the GIS interpretations and spatial information processing. Funding was from the National Science Foundation, EAR-0239655, and the US Army Cold Regions Research and Engineering Laboratory (CRREL) BT25 project, "Relationships of Soil Chemistry and Mineralogy to Cs, Pb and PGE

Distribution." The CRREL funding was provided under contract DACA42-03-P-0256. Dr. Lewis Hunter started the BT25 project while at CRREL. The authors are grateful to the Konza Prairie LTER for providing access to the study site.

References

Black, T.A., Montgomery, D.R., 1991. Sediment transport by burrowing animals, Marin county, California. Earth Surface Processes and Landforms 16, 163–172.

Briggs, J.M., Knapp, A.K., Brock, B.L., 2002. Expansion of woody plants in tallgrass prairie: a fifteen-year study of fire and fire-grazing interactions. American Midland Naturalist 147 (2), 287–294.

Brown, R.B., Cutshall, N.H., Kling, G.F., 1981a. Agricultural erosion indicated by Cs-137 redistribution 1. Levels and distribution of Cs-137 activity in soils. Soil Science Society of America Journal 45 (6), 1184–1190.

Brown, R.B., Kling, G.F., Cutshall, N.H., 1981b. Agricultural erosion indicated by Cs-137 redistribution 2. Estimates of erosion rates. Soil Science Society of America Journal 45 (6), 1191–1197.

Cambray, R.S., Playford, K., Carpenter, R.C., 1989. Radioactive Fallout in Air and Rain: results to the end of 1988. United Kingdom Atomic Energy Authority. Report no. AERE-R 10155.

Dell, C.J., Williams, M.A., Rice, C.W., 2005. Partitioning of nitrogen over five growing seasons in tallgrass prairie. Ecology 86 (5), 1280–1287.

Dietrich, W.E., Reiss, R., Hsu, M.L., Montgomery, D.R., 1995. A process-based model for colluvial soil depth and shallow landsliding using digital elevation data. Hydrological Processes 9 (3–4), 383–400.

Dietrich, W.E., Bellugi, D., Heimsath, A.M., Roering, J.J., Sklar, L., Stock, J.D., 2003. Geomorphic transport laws for predicting landscape form and dynamics. In: Wilcock, P., Iverson, R. (Eds.), Prediction in Geomorphology. American Geophysical Union, Washington, DC, pp. 103–132.

Dodds, W.K., Banks, M.K., Clenan, C.S., Rice, C.W., Sotomayor, D., Strauss, E.A., Yu, W., 1996. Biological properties of soil and subsurface sediments under abandoned pasture and cropland. Soil Biology and Biochemistry 28 (7), 837–846.

Dorr, H., Munnich, K.O., 1991. Lead and cesium transport in European forest soils. Water Air and Soil Pollution 57-8, 809–818.

Fornes, W.L., Whiting, P.J., Wilson, C.G., Matisoff, G., 2005. ^{137}Cs-derived erosion rates in an agricultural setting: the effects of model assumptions and management practices. Earth Surface Processes and Landforms 30 (9), 1181–1189.

Gabet, E.J., 2000. Gopher bioturbation: field evidence for nonlinear hillslope diffusion. Earth Surface Processes and Landforms 25, 1419–1428.

He, Q., Walling, D.E., 1996. Interpreting particle size effects in the adsorption of Cs-137 and unsupported Pb-210 by mineral soils and sediments. Journal of Environmental Radioactivity 30 (2), 117–137.

He, Q., Walling, D.E., 2003. Testing distributed soil erosion and sediment delivery models using Cs-137 measurements. Hydrological Processes 17 (5), 901–916.

Heimsath, A.M., Dietrich, W.E., Nishiizumi, K., Finkel, R.C., 1997. The soil production function and landscape equilibrium. Nature 388, 358–361.

Heimsath, A.M., Chappell, J., Spooner, N.A., Questiaux, D.G., 2002. Creeping soil. Geology 30 (2), 111–114.

Hewawasam, T., Von Blanckenburg, F., Schaller, M., Kubik, P., 2003. Increase of human over natural erosion rates in tropical highlands constrained by cosmogenic nuclides. Geology 31 (7), 597–600.

Hooke, R.L., 2000. On the history of humans as geomorphic agents. Geology 28 (9), 843–846.

Lance, J.C., McIntyre, S.C., Naney, J.W., Rousseva, S.S., 1986. Measuring sediment movement at low erosion rates using cesium-137. Soil Science Society of America Journal 50 (5), 1303–1309.

Lomenick, T.F., Tamura, T., 1965. Nautrally occuring fixation of cesium-137 on sediments of lacustrian origin. Soil Science Society of America Proceedings 29, 383–386.

Lowrance, R., McIntyre, S., Lance, C., 1988. Erosion and deposition in a field forest system estimated using cesium-137 activity. Journal of Soil and Water Conservation 43 (2), 195–199.

Macpherson, G.L., Sophocleous, M., 2004. Fast ground-water mixing and basal recharge in an unconfined, alluvial aquifer, Konza LTER Site, northeastern Kansas. Journal of Hydrology 286 (1–4), 271–299.

Martz, L.W., De Jong, E., 1987. Using cesium-137 to assess the variability of net soil erosion and its association with topography in a Canadian prairie landscape. Catena 14, 439–451.

Matisoff, G., Ketterer, M.E., Wilson, C.G., Layman, R., Whiting, P.J., 2001. Transport of rare earth element-tagged soil particles in response to thunderstorm runoff. Environmental Science and Technology 35 (16), 3356–3362.

Matisoff, G., Bonniwell, E.C., Whiting, P.J., 2002a. Radionuclides as indicators of sediment transport in agricultural watersheds that drain to Lake Erie. Journal of Environmental Quality 31 (1), 62–72.

Matisoff, G., Bonniwell, E.C., Whiting, P.J., 2002b. Soil erosion and sediment sources in an Ohio watershed using beryllium-7, cesium-137, and lead-210. Journal of Environmental Quality 31 (1), 54–61.

Montgomery, D.R., Dietrich, W.E., 1989. Source areas, drainage density, and channel initiation. Water Resources Research 25 (8), 1907–1918.

Montgomery, D.R., Dietrich, W.E., 1994. A physically-based model for the topographic control on shallow landsliding. Water Resources Research 30 (4), 1153–1171.

Navis, A., Walling, D.E., 1992. Using caesium-137 to assess sediment movement on slopes in a semiarid upland environment in Spain. Chengdu Symposium: Erosion, Debris Flows, and Environment in Mountain Regions. IAHS, pp. 129–138.

Osmundson, D.B., Ryel, R.J., Lamarra, V.L., Pitlick, J., 2002. Flow-sediment-biota relations: implications for river regulation effects on native fish abundance. Ecological Applications 12 (6), 1719–1739.

Owens, P.N., Walling, D.E., 1996. Spatial variability of caesium-137 inventories at reference sites: an example from two contrasting sites in England and Zimbabwe. Applied Radiation and Isotopes 47 (7), 699–707.

Pimentel, D., Harvey, C., Resosudarmo, P., et al., 1995. Environmental and economic costs of soil erosion and conservation benefits. Science 267 (5201), 1117–1123.

Porto, P., Walling, D.E., Tamburino, V., Callegari, G., 2003. Relating caesium-137 and soil loss from cultivated land. Catena 53 (4), 303–326.

Prosser, I.P., Dietrich, W.E., 1995. Field experiments on erosion by overland flow and their implication for a digital terrain model of channel initiation. Water Resources Research 31 (11), 2867–2876.

Quine, T.A., Govers, G., Walling, D.E., Zhang, X.B., Desmet, P.J.J., Zhang, Y.S., Vandaele, K., 1997. Erosion processes and landform evolution on agricultural land — new perspectives from caesium-137 measurements and topographic-based erosion modeling. Earth Surface Processes and Landforms 22 (9), 799–816.

Reguigui, N., Landsberger, S., 2005. Determination of soil depth profiles for Cs-137 and Pb-210 using gamma-ray spectrometry with Compton suppression. Journal of Radioanalytical and Nuclear Chemistry 264 (2), 469–476.

Roels, J.M., 1985. Estimation of soil loss at a regional scale based on plot measurements — some critical considerations. Earth Surface Processes 10, 587–595.

Roering, J.J., Almond, P., Tonkin, P., McKean, J., 2002. Soil transport driven by biological processes over millenial time scales. Geology 30 (12), 1115–1118.

Santschi, P.H., Li, Y.H., Bell, J.J., Trier, R.M., Kawtaluk, K., 1980. Pu in Coastal Marine Environments. Earth and Planetary Science Letters 51 (2), 248–265.

Seaman, J.C., Meehan, T., Bertsch, P.M., 2001. Immobilization of cesium-137 and uranium in contaminated sediments using soil amendments. Journal of Environmental Quality 30 (4), 1206–1213.

Simon, S.L., Bouville, A., Beck, H.L., 2004. The geographic distribution of radionuclide deposition across the continental US from atmospheric nuclear testing. Journal of Environmental Radioactivity 74 (1–3), 91–105.

Smith, J.T., Wright, S.M., Cross, M.A., 2004. Global analysis of the riverine transport of Sr-90 and Cs-137. Environmental Science and Technology 38 (3), 850–857.

Steegen, A., Govers, G., Takken, I., Nachtergaele, J., Poesen, J., Merckx, R., 2001. Factors controlling sediment and phosphorus export from two Belgian agricultural catchments. Journal of Environmental Quality 30 (4), 1249–1258.

Sutherland, R.A., 1994. Spatial variability of 137Cs and the influence of sampling on estimates of sediment redistribution. Catena 21, 57–71.

Sutherland, R.A., 1996. Caesium-137 soil sampling and inventory variability in reference locations: a literature survey. Hydrological Processes 10 (1), 43–53.

Tyler, A.N., Heal, K.V., 2000. Predicting areas of Cs-137 loss and accumulation in upland catchments. Water, Air, and Soil Pollution 121 (1–4), 271–288.

Van der Perk, M., Slavik, O., Fulajtar, E., 2002. Assessment of spatial variation of cesium-137 in small catchments. Journal of Environmental Quality 31 (6), 1930–1939.

VandenBygaart, A.J., King, D.J., Groenevelt, P.H., Protz, R., 1999. Cautionary notes on the assumptions made in erosion studies using fallout Cs-137 as a marker. Canadian Journal of Soil Science 79 (2), 395–397.

Wallbrink, P.J., Murray, A.S., 1996. Distribution and variability of Be-7 in soils under different surface cover conditions and its potential for describing soil redistribution processes. Water Resources Research 32 (2), 467–476.

Walling, D.E., He, Q., 1999a. Improved models for estimating soil erosion rates from cesium-137 measurements. Journal of Environmental Quality 28 (2), 611–622.

Walling, D.E., He, Q., 1999b. Using fallout lead-210 measurements to estimate soil erosion on cultivated land. Soil Science Society of America Journal 63 (5), 1404–1412.

Walling, D.E., He, Q., Blake, W., 1999. Use of Be-7 and Cs-137 measurements to document short- and medium-term rates of water-induced soil erosion on agricultural land. Water Resources Research 35 (12), 3865–3874.

Walling, D.E., Russell, M.A., Hodgkinson, R.A., Zhang, Y., 2002. Establishing sediment budgets for two small lowland agricultural catchments in the UK. Catena 47 (4), 323–353.

Wilson, C.G., Matisoff, G., Whiting, P.J., 2003. Short-term erosion rates from a Be-7 inventory balance. Earth Surface Processes and Landforms 28 (9), 967–977.

Young, A., 1960. Soil movement by denudational processes on slopes. Nature 188, 120–122.

Zhang, X.B., Quine, T.A., Walling, D.E., Li, Z., 1994. Application of the cesium-137 technique in a study of soil-erosion on gully slopes in a Yuan Area of the loess plateau near Xifeng, Gansu Province, China. Geografiska Annaler Series A-Physical Geography 76 (1–2), 103–120.